Proceedings of IASS-IWSS 2026 – September 14-18, 2026, Turin, Italy
"R-Evolution of Shapes: Sustainability, Re-Use, and New Design Paradigms"
Annual Symposium of the International Association for Shell and Spatial Structures
3rd Italian Workshop on Shell and Spatial Structures
A. Manuello Bertetto, S. Gabriele, F. Marmo, A. Micheletti (eds.)

Design and fabrication of a bistable collapsible gridshell

Davide PELLIS, Francesco LACCONE*, Luigi MALOMO, Paolo CIGNONI

*ISTI - CNR
Via G. Moruzzi 1, 56124 Pisa, Italy
francesco.laccone@isti.cnr.it

Abstract

Deployable gridshells are grid-like structures that can be deployed from a flat or collapsed configuration, simplifying the assembly and installation process. Additionally, the building elements can be fabricated using versatile manufacturing tools such as 3-axis CNC cutters. Typically, deployable gridshells are first assembled in a flat configuration and then shaped by applying increasing forces that induce elastic deformation of the beams and rotations at the joints. One of the major challenges in deploying these structures is achieving the correct opening of each joint to reach a predetermined target shape, as these structures often have many degrees of freedom. Moreover, once the desired form is achieved, the structure must be secured in place, either by locking the joint rotations or by adding bracing elements such as cables or bent beams. In this work, we address these challenges by introducing bistable collapsible gridshells structures that, due to their geometry, can collapse into a flat curve and maintain their deployed shape without the need for additional locking mechanisms. The structure can initially be assembled at rest in the planar collapsed state. Thanks to bistable equilibrium, the structure will snap into its target shape during deployment, as this represents the configuration with the minimum elastic energy among all possible deployed shapes. In the paper, we explain the geometric principles behind bistable equilibrium and design a demonstrator pavilion to showcase the potential of these structures.

Keywords: Deployable structures, Elastic grishells, Bistable structures, Digital fabrication, Architectural geometry

1. Introduction and concept

Deployable gridshells consist of networks of slender beams connected through articulated (typically scissor-type) joints, enabling the structure to be assembled in a compact or planar configuration and subsequently deployed into a target three-dimensional shape through the application of actuation forces. A landmark example is the Mannheim Multihalle designed by Frei Otto, which demonstrated the architectural potential of large-scale, doubly curved gridshells formed from initially flat configurations.

Current design approaches enable the design of gridshells that can be deployed from planar configurations [1], [2], [3], [4], [5]. Other approaches [6], [7], [8] focus instead on structures that can be deployed from compact bundles forming planar curves.

Across these methods, deployment is typically achieved by progressively increasing actuation forces applied to an initially stress-free reference configuration. The structure evolves through a sequence of intermediate states with increasing elastic energy until it reaches the desired deployed equilibrium. Once the target configuration is attained, the shape is stabilized using locking mechanisms such as fixed boundary constraints, additional bracing elements, or joint stiffening strategies.

In this work, we introduce a new class of deployable gridshells whose rest state is a compact bundle forming a planar curve and which can be deployed into a three-dimensional configuration corresponding to a local minimum of the elastic energy. Upon application of actuation forces, the elastic energy initially

Copyright © 2026 by <insert name(s) of the author(s) as listed above>
Published by the International Association for Shell and Spatial Structures (IASS) with permission.

increases and reaches a critical threshold. Beyond this point, the structure undergoes a snap-through transition into the target configuration, which can be maintained without the need for additional locking mechanisms.

This behavior arises from a geometric design principle. The beam layout approximates a surface of revolution, with the beams tracing rotationally symmetric geodesic paths. In the rest configuration, each beam corresponds to a planar curve whose curvature matches the normal curvature of the target surface. Bistability is induced because this curvature matching condition is satisfied only in the deployed configuration, where the curves are geodesics of the surface, and not in intermediate states. In the deployed configuration, the beams experience additional torsional deformation. To support this mechanism, the beams are therefore designed to be compliant in torsion, ensuring that the torsional energy contribution remains sufficiently lower than the bending energy.

2. Design

The pavilion is constructed by tracing a geodesic curve on a surface of revolution. This curve is then rotated about the axis of the surface to generate the first family of curves. The second family is obtained by reflecting these curves across the meridian plane passing through their initial point. The geodesic is computed as a polyline by forward integration, starting from a point on the first parallel and applying Clairaut's relation. A subset of the resulting geodesic network is then selected to generate the structure shown in Figure 1.

The resulting geodesic curves are then mapped into the plane, yielding curves whose pointwise curvature matches the normal curvature of the corresponding geodesics on the surface of revolution. This construction is carried out through forward integration, in which the curvature of the polyline is discretized as the inverse radius of the circumcircle defined by three consecutive vertices (previous, current, and next points). The normal curvature of the curve on the surface is computed analytically from the surface of revolution. Further details on curves tracing can be found in [8].

The beams are then constructed as follows. Since the two families of curves are symmetric with respect to meridian planes, we first select the planar curves of one family. From each planar curve, a first lamella

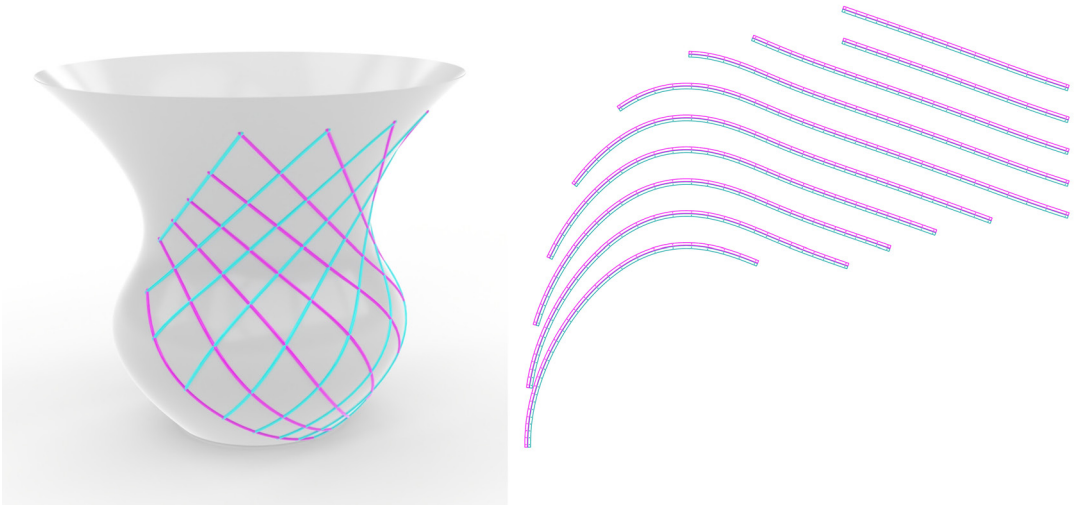

Figure 1: On the left, the pavilion is generated by a rotationally symmetric net of geodesic curves on a surface of revolution. On the right, the lamellae are generated by developing the geodesic curves onto the plane while preserving their normal curvature on the surface, and by offsetting the developed curves in two directions (only the first lamella of each family is shown; rectangular orthogonal strips are not depicted).

is obtained by offsetting the curve by 27 mm. A second, orthogonal lamella is defined as a rectangular strip with a height of 25 mm and a length equal to the arc length of the planar curve. The two lamellae are connected by L-shaped braces to form an L-shaped beam, with the orthogonal lamella obtained by bending an initially straight strip. The beam in the second family is constructed analogously, except that the first lamella is obtained by offsetting the curve by 27 mm on the opposite side relative to the first family. Along each planar curve, intersection points with curves from the other family are identified. The L-shaped braces are distributed along each segment between consecutive intersection points by subdividing the segment length into four equal parts. At intersection points, the two lamellae are also connected using L-shaped braces, which additionally function as scissor joints (Figure 2).

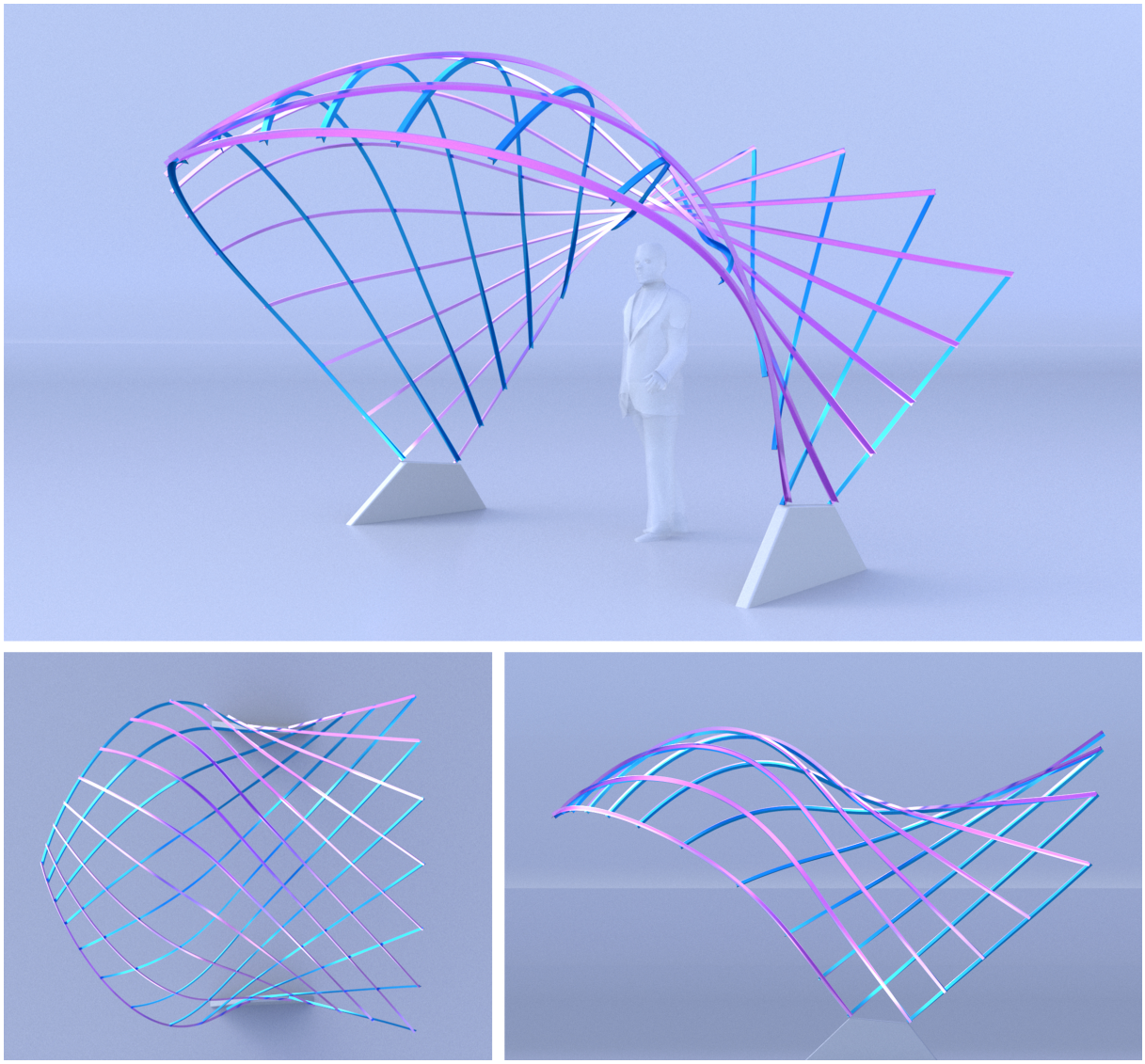

Figure 2: Preview of the deployed shape of the pavilion.

3. Fabrication

The lamellae composing the structure are CNC-cut from flat S960 steel sheets. For each beam element, the normal (orthogonal) lamella follows a prescribed curvilinear axis, while the geodesic lamella is constructed flat and elastically bent during assembly to attain the required curvature. The two lamellae are connected to form an L-shaped cross-section through discrete L-connectors located on the inner

side and fastened with M6 bolts. Scissor-like connectors are arranged between adjacent beam elements within the grid, providing a kinematic mechanism that allows relative rotation about the normal axis. This rotational degree of freedom is realized with an M8 pin acting as a planar hinge.

Beam elements are pre-assembled by elastically bending the geodesic lamella and fastening it to the normal lamella, thereby introducing stored elastic energy into the system. The grid is subsequently assembled in its compact (collapsed) configuration, characterized by staggered adjacent beams. This configuration corresponds to the first stable equilibrium state of the system, in which the total potential energy is minimized given the imposed geometric constraints, with energy stored primarily through elastic bending of the geodesic lamellae.

Deployment is achieved by applying outward forces to a pair of opposite joints, enforcing a kinematically admissible motion of the mechanism. During this process, the structure undergoes a nonlinear response, and a peak actuation force of about 10 daN is required to overcome the energy barrier associated with snap-through.

Once this energy threshold is exceeded, the structure exhibits snap-through behavior and transitions rapidly into a second stable equilibrium configuration corresponding to the fully deployed state. The structure is then positioned onto the supports.

The connection to the supports is achieved with four pinned joints located along the open boundary of the grid. These boundary conditions provide restraint against thrust forces and bending moments, ensuring global equilibrium of the deployed system.

The supports are fabricated from standard structural steel and consist of two beam segments welded to a base plate and interconnected by bracing members, which act to equilibrate horizontal thrust forces. Although the second equilibrium configuration is stable and the boundary conditions provide effective restraint, additional diagonal cable bracing is introduced across two quadrilateral cells. These elements enhance structural redundancy and provide supplementary stiffness against potential instability modes or unintended snap-back under perturbations.

The total self-weight of the structure is 66 kg, and the overall boxed dimensions are 5.15×1.7×0.025 m, allowing the system to meet standard transportation constraints in its folded configuration. Assembly and disassembly are performed manually, with the aid of viscoelastic strings used as temporary safety restraints during handling and deployment. The supports ensure sufficient dead load to counteract potential uplift effects and thereby preventing wind-induced suction.

4. Validation

A geometrically nonlinear finite element analysis of the pavilion is performed using the Abaqus software package [9] to simulate the actual behavior of the pavilion in the forming and deployment phase, and in use. The procedure is implemented as a two-step sequential analysis.

The first step models the elastic pre-bending of the geodesic lamellae prior to assembly. The lamellae are initially defined in a flat configuration, and a displacement-controlled nonlinear static analysis is carried out to map each node to its target curved geometry. Prescribed nodal displacements are applied incrementally until convergence to the final geometry is achieved (Figure 3). The resulting configuration is stored together with the corresponding residual stress field, which is transferred as initial conditions to the second step.

The second step is performed on the collapsed configuration obtained from Step 1, in which all L-shaped beam elements are already curved and assembled in their compact arrangement. The stress state from Step 1 is imported as initial stress. A nonlinear static analysis is then carried out to simulate deployment and structural response under external loading. Deployment is enforced through displacement-controlled boundary conditions applied to selected opposite boundary nodes, reproducing the physical actuation

mechanism. The solution is used to evaluate equilibrium configurations, assess stability of the compact and deployed states, and capture snap-through behavior (Figure 4).

All lamellae are discretized using four-node shell elements with reduced integration (S4R) and five integration points through the thickness. Geodesic and normal lamellae are connected using rigid connector elements representing discrete L-connectors and their local stiffening effects. Scissor joints are implemented as kinematic constraints allowing a single rotational degree of freedom about the local normal axis between adjacent lamellae. The material is defined as linear elastic and isotropic, with density $\rho = 7850\ kg/m^3$ and Young's modulus $E = 200\ GPa$.

As a result of Step 1, only geodesic lamellae are stressed due to pre-bending. A variable stress is observed due to differences in curvature and lengths of the various lamellae segments. In the final increment of Step 1, the connection to the normal lamellae are activated, so the stress redistributes among all elements.

In Step 2, it is sufficient to apply displacements along two opposing vectors to the nodes located on the same meridian line to achieve the opening.

The main results of these simulations are reported in Figure 5. The horizontal axis of the two plots represent the loading history, which is detailed as follows:

- Phase 1 takes place between increments 0 and 1 and is not shown in the plots, as its sole purpose is to introduce the initial stress state resulting from the pre-bending process.
- Between increments 1 and 4, the deployment of the pavilion is simulated. During this phase, the snap-through event is observed, and the existence of a second equilibrium configuration is verified by extending the opening beyond the target displacement.
- Between increments 4 and 5, the pavilion is allowed to settle. In this phase, the ability of the structure to recover the second equilibrium configuration is assessed by replacing the actuation constraints with spherical hinges on one side and planar roller supports on the other.
- Between increments 5 and 6, gravity loading is applied while all supports remain fixed.

The left plot in Figure 5 shows the evolution of the strain energy. It can be observed that the initial stress introduced during Phase 1 rapidly redistributes throughout the structure as soon as deployment begins. Following a peak value of approximately 250 J, the strain energy decreases to a second local minimum of about 160 J, corresponding to the deployed equilibrium configuration. Additional energy is accumulated near the end of increment 3 as the structure is pushed beyond the target configuration. However, the same energy minimum is recovered during the settling phase (between increments 4 and 5), confirming the existence of the second stable equilibrium state.

The right plot in Figure 5 reports the actuation forces required during deployment. The two curves correspond to the reaction forces measured at two nodes located symmetrically with respect to the axis of revolution and displaced along opposite directions. The reaction force approaches zero at the energy peak, corresponding to the snap-through transition. Prior to this point, an actuation force of approximately 10 daN is required to open the structure. Beyond the snap-through event, the force reverses sign and its magnitude increases, indicating that a substantially larger force is required to close the pavilion. In particular, closure requires forces exceeding 30 daN. This characteristic is advantageous from a safety perspective, as the energy barrier associated with closure is significantly higher than that associated with opening. Starting from increment 4, the actuation joint represented by the orange curve is converted into a roller support, enabling the structure to converge to the second equilibrium configuration.

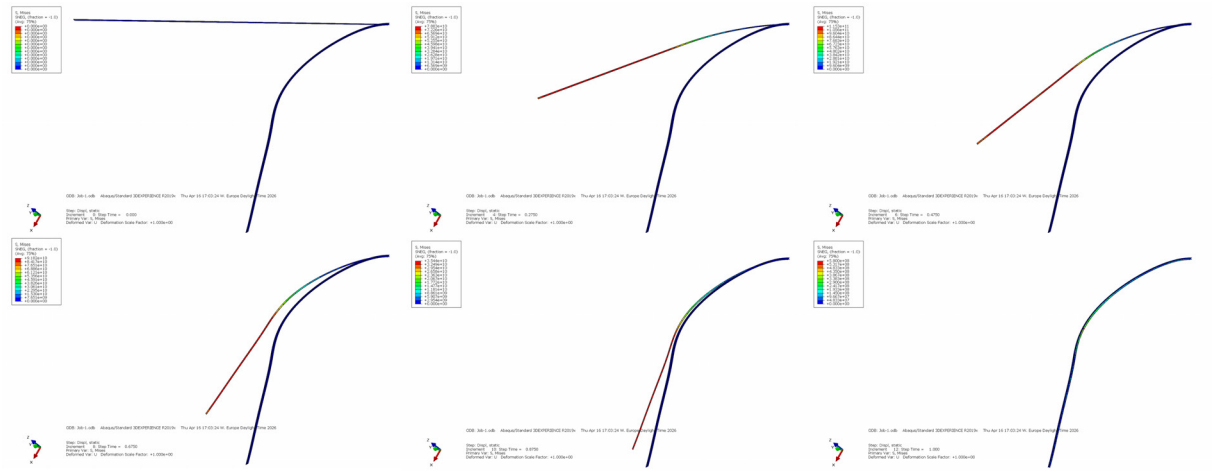

Figure 3: Step 1 of the finite element analysis of the pavilion. The geodesic lamellae start from flat configuration and are displaced to match the target curvature, and later linked to the normal lamellae.

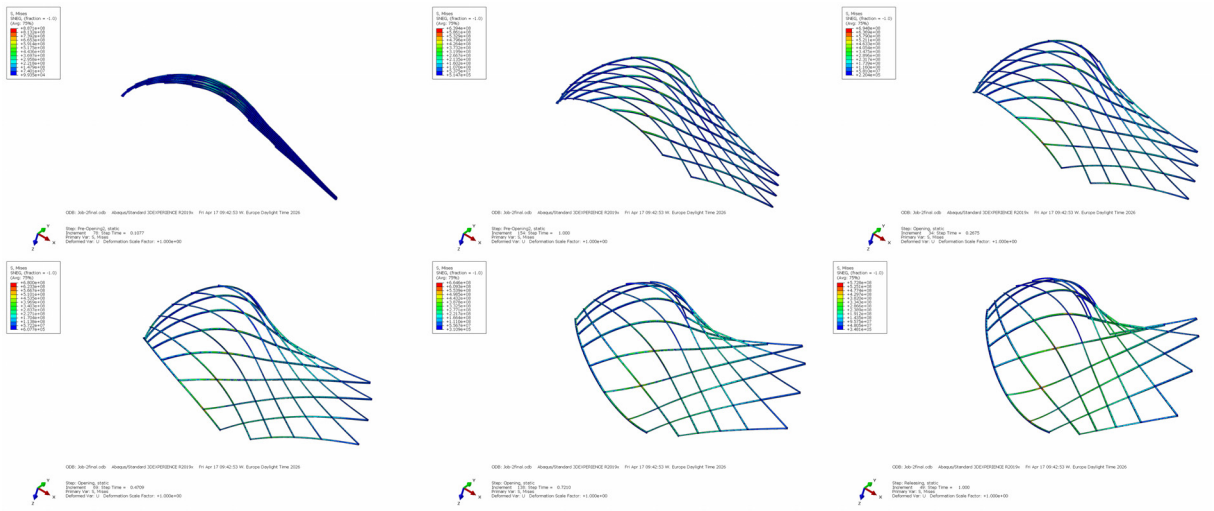

Figure 4: Step 2 of the finite element analysis of the pavilion. The structure is actuated by displacing opposite nodes.

5. Conclusions

This paper presented a bistable collapsible pavilion and demonstrated the feasibility of employing its forming principle in the design of lightweight bending-active structures. The pavilion shows how target geometries can be achieved through the appropriate variation of grid geometric parameters while preserving the bistable behavior of the system.

The results highlight the potential of combining bending-active principles with deployable and bistable mechanisms to create lightweight structures capable of transitioning between distinct equilibrium configurations. The successful realization of the pavilion prototype demonstrates the applicability of this design strategy at the architectural scale and suggests new opportunities for deployable structures that integrate shape formation, structural efficiency, and compact storage within a single system.

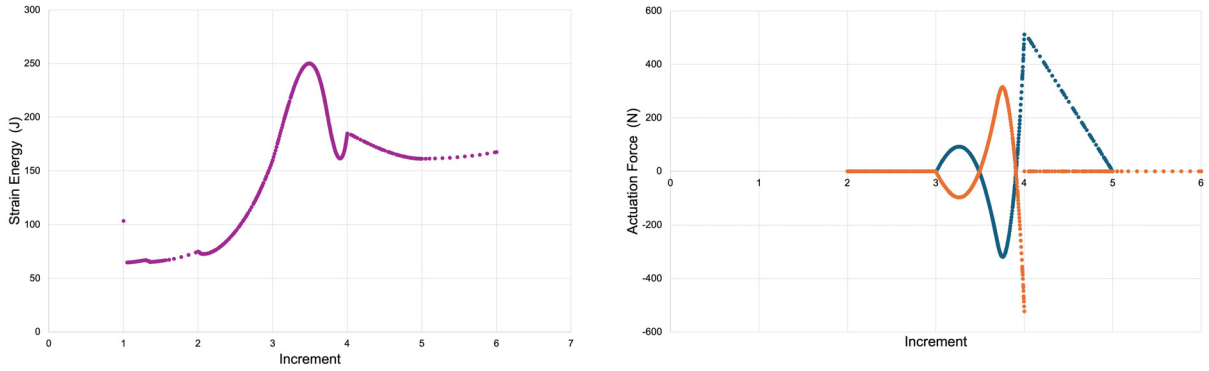

Figure 5: Simulation results: on the left, strain energy plot; on the right actuation forces.

Acknowledgements

The authors acknowledge Moni2BSafe for supporting the structural monitoring of the Pavilion during deployment and exhibition time.

References

[1] J. Panetta, M. Konaković-Luković, F. Isvoranu, E. Bouleau, and M. Pauly, "X-shells: A new class of deployable beam structures," *ACM Trans. Graph.*, vol. 38, no. 4, 83:1–15, 2019.

[2] Q. Becker, S. Suzuki, Y. Ren, D. Pellis, J. Panetta, and M. Pauly, "C-shells: Deployable gridshells with curved beams," *ACM Trans. Graph.*, vol. 42, no. 6, 181:1–17, 2023.

[3] S. Pillwein, K. Leimer, M. Birsak, and P. Musialski, "On elastic geodesic grids and their planar to spatial deployment," *ACM Trans. Graph.*, vol. 39, no. 4, 125:1–12, 2020.

[4] E. Soriano, R. Sastre, and D. Boixader, "G-shells: Flat collapsible geodesic mechanisms for gridshells," in *Proc. of IASS annual symposia 2019*, Int. Ass. for Shell and Spatial Structures (IASS), 2019, pp. 1–8.

[5] J. Schikore, "Morphology of kinetic asymptotic grids," in *Towards Radical Regeneration: Design Modelling Symposium Berlin 2022*, Springer Nature, 2022, p. 374.

[6] X. Tellier, "Bundling elastic gridshells with alignable nets. part i: Analytical approach," *Automation in Construction*, vol. 141, p. 104 291, 2022.

[7] D. Liu, D. Pellis, Y.-C. Chiang, F. Rist, J. Wallner, and H. Pottmann, "Deployable strip structures," *ACM Trans. Graph.*, vol. 42, no. 4, 103:1–16, 2023.

[8] D. Pellis, "Alignable lamella gridshells," *ACM Trans. Graph.*, vol. 43, no. 6, 183:1–21, 2021.

[9] D. Systèmes, *"Abaqus analysis user's manual"*. Simulia Corp. Providence, RI, USA, vol. 40, 2022.